The Iraqi Journal For Mechanical And Material Engineering, Vol.9, No.3, 2009

THE EFFECT OF SPARK PLUG LOCATION ON CYLINDER PRESSURE, TEMPERATURE FIELD AND POLLUTANTS CONCENTRATION

Dr. Haroun A.K. Shahad* Dr. Tahseen AL-Hattab Intesar Fadhil Hachim***
*** Department of Mechanical Engineering / College of Engineering / Babylon University**
****Department of Electrochemical Engineering / College of Engineering / Babylon University**

ABSTRACT

The growing concern about the fast depletion of hydrocarbon-based fuels and the environmental pollution caused by their combustion has been a compelling incentive to all researchers to study the effective parameters on the combustion processes. One of these parameters is the effect of spark plug location. Keeping this in mind, a mathematical model for the power cycle in a 4-stroke spark ignition engine was developed using quasi-dimensional cycle simulation. The model takes in to consideration mass and energy conservation in the engine cylinder. The model calculates instantaneous variation in gas thermodynamic states, gas properties, cylinder pressure, burnt temperature, turbulent flame speed, flame radius, and pollutants formation. Three spark plug location are used, namely,

1- The spark plug at the center.
2- The spark plug is at a distant ratio (0.4).
3- The spark plug is at a distant ratio (0.3).

It is found that the position of the spark plug have a strong effect on the pressure, temperature, flame speed, and pollutants concentration. Shifting the spark plug from central position towards the wall reduces all studied parameters.

الخلاصة

إن ازدياد القلق من النضوب السريع لمصادر الطاقة وخاصة الاحفورية منها والتأثيرالسيئ الذي تحدثه على البيئة وخاصة عند احتراقها كان لهما الأثر الكبير في تحفيز الباحثين لدراسة العوامل المؤثرة على عملية الاحتراق ومنها دراسة تأثير موقع شمعة القدح على عملية الاحتراق والملوثات المتبقية. في ظل هذه المعطيات تم بناء برنامج لتمثيل العمليات التي تحدث داخل اسطوانة المحرك وذلك بتطوير نموذج رياضي شبه بعدي لمحرك احتراق داخلي رباعي الشوط يعمل بالشرارة، معتمدا على قانوني حفظ الطاقة والكتلة. يهدف النموذج دراسة التغيرات اللحظية في الخواص الثرموديناميكية للغازات، درجة الحرارة، الضغط ، سرعة تقدم اللهب والملوثات. حيث تم دراسة ثلاث مواقع لشمعة القدح وهي:

1- عندما تكون شمعة القدح في المركز.
2- عندما تكون شمعة القدح على مسافة مساوية إلى0.4 من قطر الاسطوانة.
3- عندما تكون شمعة القدح على مسافة مساوية إلى0.3 من قطر الاسطوانة.

وقد وجد إن تغير موقع شمعة القدح له تأثير كبير على الضغط، درجة الحرارة، سرعة تقدم اللهب و الملوثات. حيث إن تغير موقعه من المركز باتجاه الجدار يؤدي إلى تناقص جميع المتغيرات المدروسة.

1. INTRODUCTION

In recent years the combined effects of environmental legislation and the energy saving demands have led to a major expansion of research and development work in order to make better fuel combustion, and to reduce pollutants emission. Combustion is important for its impact on several other engine characteristics or requirements. The process by which the engine's emissions within the cylinder are closely linked with the combustion process. The anti-knock and volatility requirements of the fuel are dictated by the engine combustion process. Even the breathing of the engine, and hence its power, are affected by what the designer must do to achieve a good combustion process. It is not surprising, therefore, that understanding the engine combustion process, and modeling that process from a fundamental perspective, are such important topics for the engine research. So analysis of in-cylinder temperature and pressure characteristics during combustion has become an important research field so far, because it must proceed to analyze combustion characteristics accurately (Heywood [1994]).

In this context many codes were developed to simulate internal combustion engines, such as quasi-dimensional models and two or three, dimensional codes, which are classified as CFD codes. Although the CFD codes permit very good simulation of physical phenomena involved in engines, but the long time needed for calculation is one of their shortages. In opposition the quasi-dimensional models are fast executing models, which can be used extensively by automotive industry in order to develop engine design and filling and emptying operation very fast (Razavi [2002]). The purpose of this work is to study the effect of spark plug location on cylinder pressure, temperature field and pollutants concentration in a spark ignition engine.

2. THE MATHEMATICAL MODEL

In this model the SI engine cycle is treated as a sequence of five processes: intake, compression, combustion, expansion, and exhaust. The model developed in this work is concerned with the processes of the closed cycle (power cycle) which are compression, combustion, and expansion.

2.1 Compression Process

The following assumptions have been made during the modeling of compression stroke:

(1)The mixing between fresh charge and residual gases is perfect.

(2)No chemical reaction occurs during compression. The calculation procedure starts with the trapped mass of fuel, air and residuals. The pressure and temperature during this process are then modeled using the first law of thermodynamics and the equation of state; which lead to the following equations:

$$\frac{dT}{dt} = T \cdot \left[\frac{1}{P} \cdot \frac{dP}{dt} + \frac{1}{V} \cdot \frac{dV}{dt} \right] \qquad (1)$$

$$\frac{dP}{dt}=\left[-\left(1+\frac{R_{mol}}{C_V(T)}\right).P.\frac{dV}{dt}+\frac{R_{mol}}{C_V(T)}.\frac{dQ_{ht}}{dt}\right]/V \qquad (2)$$

2.2 Combustion Process

The combustion process is simulated by a two zone quasi-dimensional model. The combustion chamber is divided into two volumes: the unburned zone composed of air, fuel, and residuals and burned zone composed of combustion products. The energy equation for each zone is applied to a closed system. The Woshni correlation is used to calculate the rate of heat transfer from engine. The numerical method for solving differential equations in this work is Range-Kutta of fourth order.

The following assumptions have been made during the modelling of combustion process:

(1)The pressure is assumed to be uniform in the chamber.

(2)The flame surface is located just in front of the flame, and thus, there is no heat transfer between the burned and unburned mixture.

(3)The flow leakage through valves and past the piston rings is neglected.

Ignition Model

In the present work, the ignition model used the same approach as (Zhichao[2003]), where the ignition kernel is assumed to be spherical during the initial ignition process. When the kernel grows, the particles move outwards radially from the spark plug electrodes. The ignition particle's speed, i.e., the kernel growth rate, is influenced by the flow turbulence and air-fuel mixture stoichiometry.

A thermodynamic system of an ignition kernel is used to analyze the flame kernel growth rate. The following assumptions are made in the calculations:

1. The calculation starts at 1μs after the breakdown period. The ignition kernel is assumed to be spherical. Its radius is assumed to be 0.5mm at this time.
2. The ignition kernel flame is very thin and separates the burned and unburned gas.
3. The ignition kernel surface is located just in front of the flame, and thus, there is no heat transfer between the kernel and unburned gas.
4. The pressure is uniform inside the kernel and outside the kernel.
5. The temperature inside the kernel is uniform.

The ignition kernel mass-burning rate $M_k^{\bullet}$, which is also the increase in the flame kernel mass, is written as;

$$M_k^{\bullet}=\frac{dM_k}{dt}=\rho_u.A_K.S_T \qquad (3)$$

Where; ρ_u unburned gas density [kg/m³].

A_K flame kernel surface area [m²].

S_T turbulent speed [m/s].

In addition, using $M_k=\rho_k.V_k$, the mass-burning rate can be rewritten as;

$$\frac{dM_k}{dt}=\frac{d(\rho_k.V_k)}{dt}=\rho_k.\frac{dV_k}{dt}+V_k.\frac{d\rho_k}{dt}=\rho_u.A_k.S_T \qquad (4)$$

Where; ρ_k gas density [kg/m³].

V_k kernel volume [m³].

Utilizing the ideal gas law($P = \rho.R.T$);

$$\frac{1}{\rho_k}.\frac{d\rho_k}{dt} = \frac{1}{P}.\frac{dP}{dt} - \frac{1}{T_k}.\frac{dT_k}{dt} \tag{5}$$

The following equation is obtained;

$$\frac{dV_k}{dt} = \frac{\rho_u}{\rho_k}.A_k.S_T + V_k(\frac{1}{T_k}.\frac{dT_k}{dt} - \frac{1}{P}.\frac{dP}{dt}) \tag{6}$$

Normalizing the volume increase to the flame kernel surface area A_k, the change in flame kernel radius can be obtained as;

$$\frac{dr_k}{dt} = \frac{\rho_u}{\rho_k}.S_T + \frac{V_k}{A_k}(\frac{1}{T_k}.\frac{dT_k}{dt} - \frac{1}{P}.\frac{dP}{dt}) \tag{7}$$

(Zhichao[2003]), assumes that during the ignition process, the pressure increase due to the combustion is negligible, and the temperature inside the kernel is spatially uniform and equal to the adiabatic flame temperature of the fuel-air mixture.
With these two assumptions, the kernel growth rate is simplified as;

$$\frac{dr_k}{dt} = \frac{\rho_u}{\rho_k}.S_T \tag{8}$$

This flame kernel growth is initially laminar like, at least at low to mid-speed engine operating conditions (Heywood [1988]).

Flame Propagation Model

This model attempt to predict the burning rate as a function of turbulent flame speed (S_T) and instantaneous flame area (A_f). This approach allows the calculated burning rates to respond to cylinder geometry and flows.

The mass burning rate is predicted by the following formula (Heywood [1988]);

$$\frac{dM_b}{dt} = A_f \cdot \rho u \cdot S_T \tag{9}$$

Where;

M_b mass of burnt gases [kg].

t time [sec].

But $M_b = \rho_b.V_b$ (10)

The mass-burning rate can be rewritten as;

$$\frac{dM_b}{dt} = \frac{d(\rho_b.V_b)}{dt} = \rho_b.\frac{dV_b}{dt} + V_b.\frac{d\rho_b}{dt} = \rho_u.A_f.S_T \quad (11)$$

Where; ρ_b burnt gas density [kg/m³].
V_b enflamed volume [m³].
Utilizing the ideal gas law($P = \rho.R.T$);

$$\frac{1}{\rho_b}.\frac{d\rho_b}{dt} = \frac{1}{P}.\frac{dP}{dt} - \frac{1}{T_b}.\frac{dT_b}{dt} \quad (12)$$

The following equation is obtained;

$$\frac{dV_b}{dt} = \frac{\rho_u}{\rho_b}.A_f.S_T + V_b(\frac{1}{T_b}.\frac{dT_b}{dt} - \frac{1}{P}.\frac{dP}{dt}) \quad (13)$$

Normalizing the volume increase to the flame front area, the change in flame radius can be obtained as;

$$\frac{dr_f}{dt} = \frac{\rho_u}{\rho_b}.S_T + \frac{V_b}{A_f}(\frac{1}{T_b}.\frac{dT_b}{dt} - \frac{1}{P}.\frac{dP}{dt}) \quad (14)$$

The first law of thermodynamic for a closed system is:

$$\frac{dQ_{ht}}{dt} = \frac{dE}{dt} + \frac{dW}{dt} \quad \text{[kJ/sec]} \quad (15)$$

Where; dQ_{ht} total heat transfer rate to the cylinder wall [kJ].
dE change of internal energy in the system [kJ].
dW work transfer from the system [kJ].

$$\frac{dQ_{ht}}{dt} = \frac{dQ_b}{dt} + \frac{dQ_u}{dt} \quad (16)$$

$$\frac{dQ_b}{dt} = A_b.h_{cb}.(T_b - T_w) + A_b.\sigma.\varepsilon_g(T_b - T_w) \quad (17)$$

$$\frac{dQ_u}{dt} = A_u.h_{cu}.(T_u - T_w) \quad (18)$$

The total internal energy of cylinder contents is;

$$\frac{dE}{dt} = \frac{dE_b}{dt} + \frac{dE_u}{dt} \quad (19)$$

$$\frac{dE_b}{dt} = N_b.\frac{de_b(T_b)}{dt} + e_b.\frac{dN_b}{dt} \quad (20)$$

$$\frac{dE_u}{dt} = N_u.\frac{de_u(T_u)}{dt} + e_u.\frac{dN_u}{dt} \quad (21)$$

And from definition of specific heat at constant volume;

$$C_V(T) = \frac{de(T)}{dT} \quad (22)$$

Now;

$$\frac{dM_b}{dt} = -\frac{dM_u}{dt} \quad (23)$$

$$Mw_b.\frac{dN_b}{dt} = -Mw_u\frac{dN_u}{dt} \quad (24)$$

Where ; Mw_u molecular weight of un burnt mixture [kg/Kmol].

Mw_b molecular weight of burnt mixture [kg/Kmol].

Thus equation (19) becomes after rearrangement;

$$\frac{dE}{dt} = \left(e_b(T_b) - e_u(T_u).\frac{Mw_b}{Mw_u}\right)\frac{dN_b}{dt} + N_b.C_{Vb}(T_b).\frac{dT_b}{dt} + N_u.C_{Vu}(T_u).\frac{dT_u}{dt} \quad (25)$$

The work transfer from the system is;

$$\frac{dW}{dt} = P.\frac{dV}{dt} \quad (26)$$

$$\frac{dV}{dt} = \frac{dV_u}{dt} + \frac{dV_b}{dt} \quad (27)$$

The differentiation of the equation of state with respect to time gives;

$$\frac{dV_u}{dt} = \frac{R_{mol}.N_u}{P}.\frac{dT_u}{dt} + \frac{R_{mol}.T_u}{P}.\frac{dN_u}{dt} - \frac{V_u}{P}.\frac{dP}{dt} \quad (28)$$

$$\frac{dV_b}{dt} = \frac{R_{mol}.N_b}{P}.\frac{dT_b}{dt} + \frac{R_{mol}.T_b}{P}.\frac{dN_b}{dt} - \frac{V_b}{P}.\frac{dP}{dt} \quad (29)$$

$$\frac{dV}{dt}=(\frac{V_b}{N_b}-\frac{V_u}{N_u}.\frac{Mw_b}{Mw_u})\frac{dN_b}{dt}+\frac{R_{mol}.N_u}{P}.\frac{dT_u}{dt}+\frac{R_{mol}.N_b}{P}.\frac{dT_b}{dt}-\frac{V}{P}.\frac{dP}{dt} \quad (30)$$

Applying the first law of thermodynamic for unburned zone;

$$\frac{dQ_u}{dt}=\frac{dE_u}{dt}+P\frac{dV_u}{dt} \quad (31)$$

The combination of equations (21), (28), and (31) gives;

$$\frac{dT_u}{dt}=\frac{1}{N_u.C_{Pu}(T_u)}.\frac{dQ_u}{dt}+\frac{V_u}{N_u.C_{Pu}(T_u)}.\frac{dP}{dt} \quad (32)$$

A combination of equations (28), and (32) after rearrangement gives;

$$\frac{dT_b}{dt}=\frac{P}{N_bR_{mol}}\left[\frac{dV}{dt}-\left(\frac{R_{mol}.T_b}{P}-\frac{R_{mol}.T_u}{P}.\frac{Mw_b}{Mw_u}\right)\frac{dN_b}{dt}-\frac{V_u.R_{mol}}{P.C_{Pu}}.\frac{dP}{dt}-\frac{R_{mol}}{P.C_{Pu}}.\frac{dQ_u}{dt}+\frac{V}{P}.\frac{dP}{dt}\right] \quad (33)$$

Finally a combination of equations (23), (32), and (33) after rearrangement gives;

$$\frac{dP}{dt}=\frac{-\left[P\frac{dV}{dt}\left(1+\frac{C_{Vb}}{R_{mol}}\right)+\left(\frac{C_{Vu}}{CP_u}-\frac{C_{Vb}}{CP_u}\right)\frac{dQ_u}{dt}+\left[e_b-e_u\frac{Mw_b}{Mw_u}-C_{Vb}\left(T_b-T_u\frac{Mw_b}{Mw_u}\right)\right]\frac{dN_b}{dt}-\frac{dQ_{ht}}{dt}\right]}{\left[\frac{C_{Vu}(T_u)}{C_{Pu}(T_u)}.V_u-\frac{C_{Vb}(T_b)}{C_{Pu}(T_u)}.V_u+\frac{C_{Vb}(T_b)}{R_{mol}}.V\right]} \quad (34)$$

Equations (32), (33), and (34) are solved by Runge-Kutta method to calculate the unburned zone temperature, the burned zone temperature, and the cylinder pressure respectively during each time step.

2.3 Expansion Process

Once the combustion process is completed, the combustion chamber is assumed to be formed of a single zone with uniform pressure and temperature. The Runge-Kutta method is used to solve the pressure and temperature differential equations.

$$\frac{dT}{dt}=T.\left[\frac{1}{P}.\frac{dP}{dt}+\frac{1}{V}\frac{dV}{dt}\right] \quad (35)$$

$$\frac{dP}{dt}=\left[-\left(1+\frac{R_{mol}}{C_V(T)}\right).P.\frac{dV}{dt}+\frac{R_{mol}}{C_V(T)}.\frac{dQ_{ht}}{dt}\right] \quad (36)$$

2.4 NOx Formation

It is assumed that only 12 species are present in the combustion products both inside the cylinder as well as the exhaust. These are: H_2O, H_2 , OH, H , N_2, NO, CO_2 , CO, CO_2, O_2 , O , Ar.

The governing equations for the mechanism of NO formation are (Lavoie et. al. [1970]).

$$N + NO \leftrightarrow N_2 + O \qquad K_{1f} = 3.1*10^{10} \exp\left(\frac{-160}{T}\right) [m^3 / Kmol.S] \tag{37}$$

$$N + O_2 \leftrightarrow NO + O \qquad K_{2f} = 6.4*10^6 * T * \exp\left(\frac{-3125}{T}\right) [m^3 / Kmol.S] \tag{38}$$

$$N + OH \leftrightarrow NO + H \qquad K_{3f} = 4.2*10^{10} \quad [m^3 / Kmol.S] \tag{39}$$

Where; K_{if} denotes the forward rate constant for the ith reaction.

Let K_{ib} the backward rate constant for the ith reaction and R_i the "One-way" equilibrium rate for the ith reaction then;

$$\alpha_{NO} = \frac{[NO]}{[NO]_e} \tag{40}$$

$$\beta_N = \frac{[N]}{[N]_e} \tag{41}$$

From equation (37) the net rate is;

$$-K_{1f}[N][NO]_e + K_1 b[N_2][O] = -\alpha_{NO}.\beta_N[N]_e.[NO]_e K_{1f} + K_1 b[N_2][O]_e \tag{42}$$

But

$$K_1 f[N]_e[NO]_e = K_1 b[N_2]_e[O]_e = R_1 \tag{43}$$

So that the net rate becomes:

$$K_1 f[N]\ [NO]_e + K_1 b[N_2][O]\ = -\alpha_{NO}\beta_N.R_1 + R_1 \tag{44}$$

Using the similar term for equations (38), and (39), involving NO, then;

$$\frac{1}{Ven}.\frac{d([NO].Ven)}{dt} = -\alpha_{NO}(\beta_N R_1 + R_2 + R_3) + R_1 + \beta_N(R_2 + R_3) \tag{45}$$

Also using equations (35), (36), and (37) the following relationship is obtained;

$$\frac{1}{Ven}.\frac{d([N].Ven)}{dt} = -\beta_{NO}(\alpha_{NO}R_1 + R_2 + R_3) + R_1 + \alpha_{NO}(R_2 + R_3) \quad (46)$$

Lavoie [1970] found that a finite time is required for the reactions to reach their equilibrium values; this is called Relaxation time. The relaxation times are several orders of magnitude for the formation of atomic Nitrogen than those of NO, and hence it can be assumed that [N] values are at steady state, which means that the right hand sides of equation (17) can be set to equal zero, therefore;

$$\beta_N = \frac{R_1 + \alpha_{NO}(R_2 + R_3)}{\alpha_{NO}R_1 + R_2 + R_3} \quad (47)$$

Substituting for β_N in equation (16), gives;

$$\frac{1}{Ven}.\frac{d([NO].Ven)}{dt} = 2(1-\alpha_{NO}^2)\left[\frac{R_1}{(1+\alpha_{NO}(R_1/(R_2+R_3)))}\right] \quad (48)$$

Which is the final rate equation for [NO].

2.5 Carbon Monoxide Formation

The formation of CO inside the cylinder is assumed to be at equilibrium condition up to the peak value. After that, the concentration of CO is assumed to lie between the peak equilibrium and the current equilibrium.

This is because, at low temperature during the expansion process, the actual chemical reaction rates for the formation of CO lag behind the equilibrium value leading to a higher value than obtained at equilibrium.

The principal CO oxidation reaction in hydrocarbon-air flame is;

$$CO + OH \leftrightarrow CO_2 + H \quad (49)$$

Heywood [1988], showed that the rate constant for this reactions is;

$$K_f = 6.76*10^{10}\exp\left(\frac{T}{1102}\right) \qquad [cm^3/g.mol] \quad (50)$$

Thus;

$$\frac{1}{Ven}.\frac{d([CO].Ven)}{dt} = K_f[CO].[OH] - K_b[CO_2][H] \quad (51)$$

Where V_{en} is the enflamed volume using;

$$\alpha_e = \frac{[CO]}{[CO]_e} \quad (52)$$

$$\delta_e = \frac{[CO_2]}{[CO_2]_e} \quad (53)$$

$$\beta_e = \frac{[OH]}{[OH]_e} \tag{54}$$

$$\beta_e = \frac{[OH]}{[OH]_e} \tag{55}$$

$$\sigma_e = \frac{[H]}{[H]_e} \tag{56}$$

Therefore;

$$\frac{1}{Ven}.\frac{d([CO].Ven)}{dt} = (\alpha_e.\beta_e - \delta_e.\sigma_e)R_f \tag{57}$$

Where; R_f one – way equilibrium rate.

Since the actual value of CO lies between the peak and exhaust equilibrium values, a multiplication factor called "COFAC" is introduced to obtain amore realistic value at exhaust. Gupta [2003] used the following relation to calculate the concentration of CO;

$$X_{CO} = X_{COeq} + COFAC.(X_{CO\max} - X_{COeq}) \tag{58}$$

Where; X_{CO} corrected concentration of CO.

X_{COeq} concentration of CO at equilibrium.

X_{max} maximum value of CO concentration at equilibrium condition.

$COEAC$ scale factor for CO formation.

The value of COFAC is adjusted with experimental results and found to be equals approximately 0.6 (Gupta [2003]).

RESULT AND DISCUSSION

The result showed that the spark plug location has a significant effect on both combustion process and emission characteristics of the engine and has to be carefully designed.

Before proceeding with the discussion it would be appropriate to define the terms used in the program. (a/B) is a non-dimensional parameter referring to the ratio of the distance between the spark plug location from the nearest wall to the cylinder diameter. Relocating the spark plug from the center to the side is far more effective in increasing burn duration which affects incylinder pressure, temperature, and NOx and CO emissions as will be shown below at different spark plug location.

Figure (1) ((a), (b), and (c)) show the variation of the cylinder pressure with crank angle. In general the behavior for these figures is the same except the difference in the value of peak pressure which depend on spark plug location. These figures show that as

the spark is shifted from the center (i.e. (a/B) = 0.5), to the peripheral position (i.e. (a/B) = 0.4, 0.3), the maximum pressure decrease because the increased percentage in heat loss as the combustion duration increased. The heat losses are also increased due to longer contact period between hot gasses and cylinder walls.

Figure (2) ((a), (b), and (c)) show that the flame grows roughly spherically and steadily from the time of the spark discharge. The burned gas temperature and the associated pressure rise due to combustion increase significantly as the flame front has traveled through the combustion chamber. The maximum temperature and pressure occurs close to the time that the flame makes contact with the cylinder wall. At this time there is a direct contact between the hot gases and the cylinder liner. This causes a large increase in the rate of heat loss. These figures show that as the spark is shifted from the center (i.e. (a/B) = 0.5), to the peripheral position (i.e. (a/B) = 0.4, 0.3), the maximum temperature decrease.

Figure (3) ((a), (b), and (c)) show the flame speed contours. The flame speed decreases as the flame radius increase. This is due to the increase in cylinder pressure and temperature which increase the density of the unburnt mixture.
The presence of the cylinder wall causes a decrease in flame speed as the flame gets closer to the wall.
The flame speed also decreases as the spark plug is shifted towards the wall due to the quenching effect of the wall.
These figures show that as the spark is shifted from the center (i.e. (a/B) = 0.5), to the peripheral position (i.e. (a/B) = 0.4, 0.3), the flame speed decrease. This creates a favorable condition for the increasing of ignition lag and decrease in the flame speed.

Figure (4) ((a), (b), and (c)) show the variation of NOx and CO concentrations with crank angle. The NOx and CO concentrations increase sharply with time and then freeze due to temperature drop where the reaction cannot proceed.
These figures show that as the spark is shifted from the center (i.e. (a/B) = 0.5), to the peripheral position (i.e. (a/B) = 0.4, 0.3), the NOx and CO concentrations decrease. The decrease in the concentration of CO may be attributed to the drop in cylinder temperature which in turn affects the dissociation process of CO_2. On the other hand the drop in cylinder temperature reduces the NO concentration.
From the emission point of view, the location ((a/B) = 0.3) is most favorable.

Figure (5) shows the effect of spark plug location on the combustion duration at different compression ratios. The graph has been plotted for Φ =1 and engine speed 2500rpm. The figure shows that the combustion duration decreases as the compression ratio is increased and as the spark plug location is shifted towards the cylinder center line. The increase in compression ratio and the movement of the spark plug towards the center line cause an increase in cylinder temperature i.e an increase in unburnt zone temperature and this reduces the burnt duration.

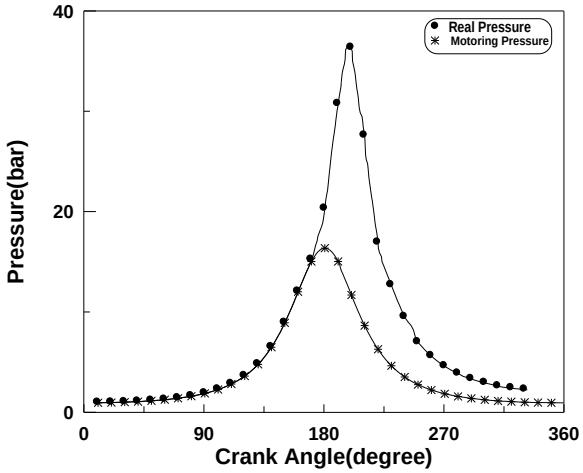

(a): Central location

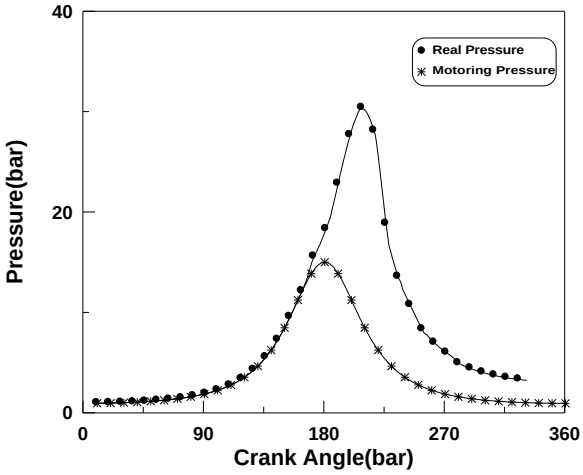

(b): (a/B) = 0.4.

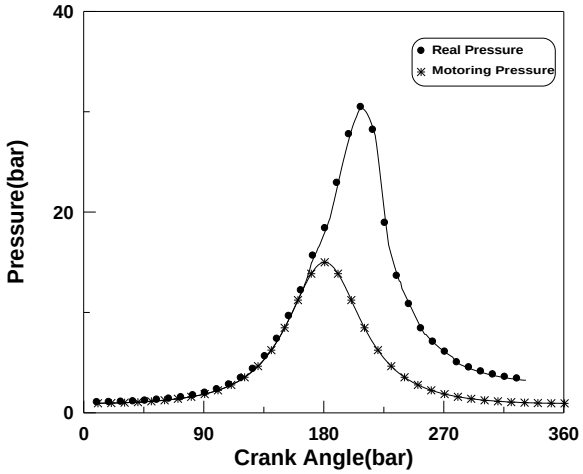

(c): (a/B) = 0.3.

Fig. (1): Variation of cylinder pressure with crank angle.
Equivalence ratio:1.0, Compression ratio: 7.5, Engine speed: 1500, Spark timing: 20BTDC)(

(a): central location

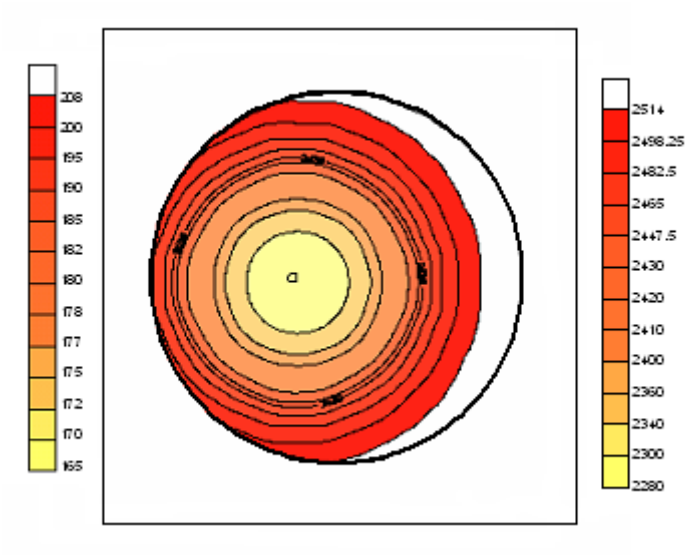

(b): (a/B) = 0.4.

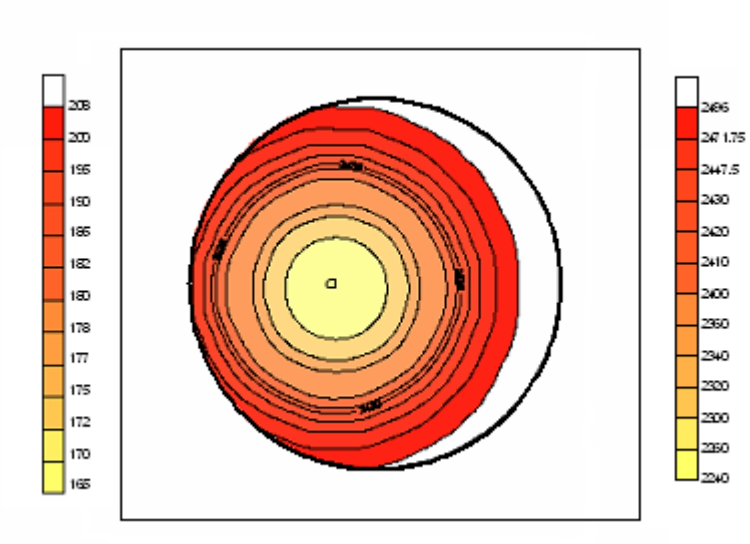

(c): (a/B) = 0.3.

Fig. (2): Temperature contours
(Equivalence ratio:1.0, Compression ratio: 7.5, Engine speed: 1500,Spark timing: 20 BTDC)

(a): central location

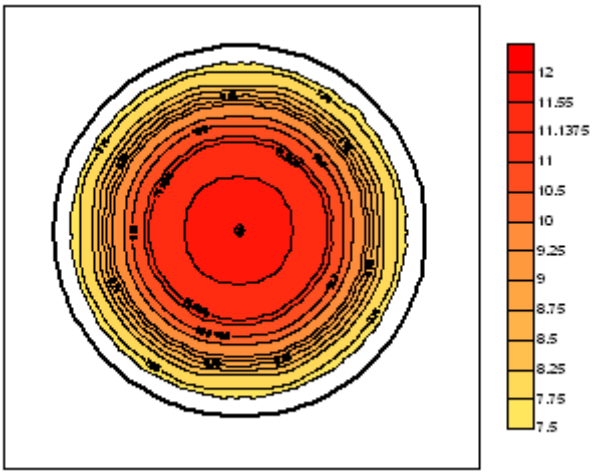

(b): (a/B) = 0.4.

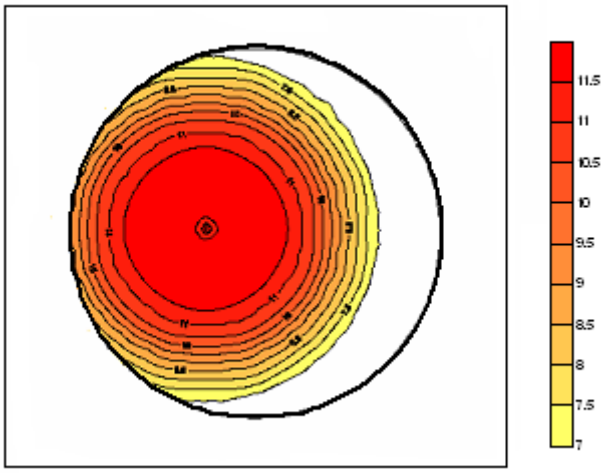

(c): (a/B) = 0.3.

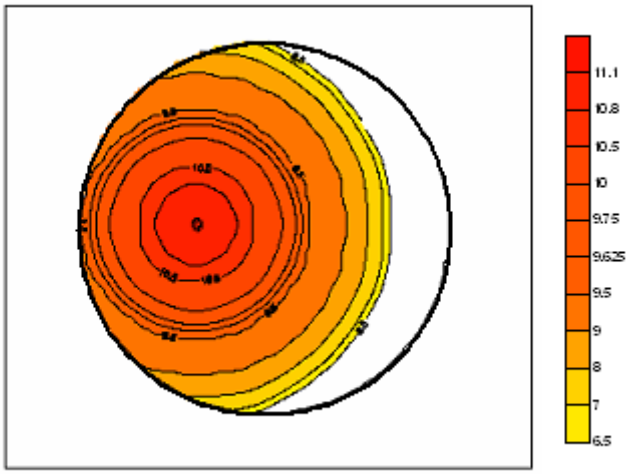

Fig. (3): Flame speed contours
(Equivalence ratio:1.0, Compression ratio: 7.5, Engine speed: 1500, Spark timing: 20 BTDC).

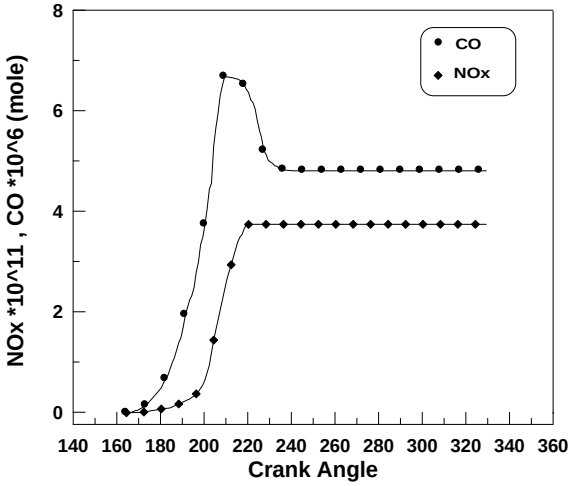

(a): central location

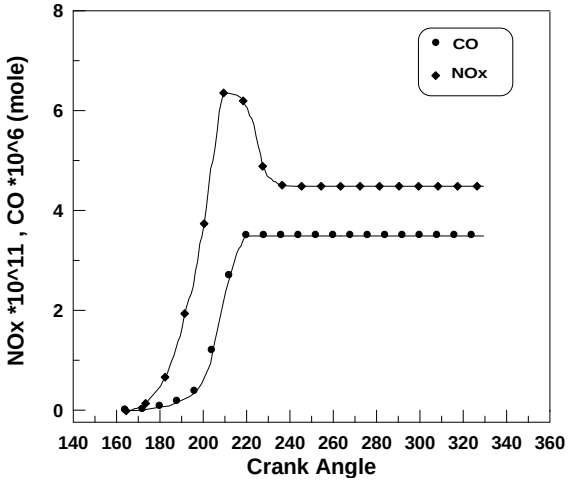

(b): (a/B) = 0.4.

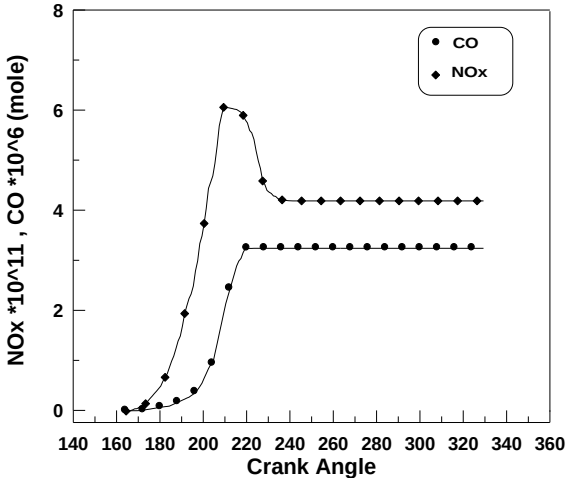

(c): (a/B) = 0.3.

Fig. (4): Variation of concentration of NOx and CO with crank angle.
(Equivalence ratio:1.0, Compression ratio: 7.5, Engine speed: 1500, Spark timing: 20 BTDC).

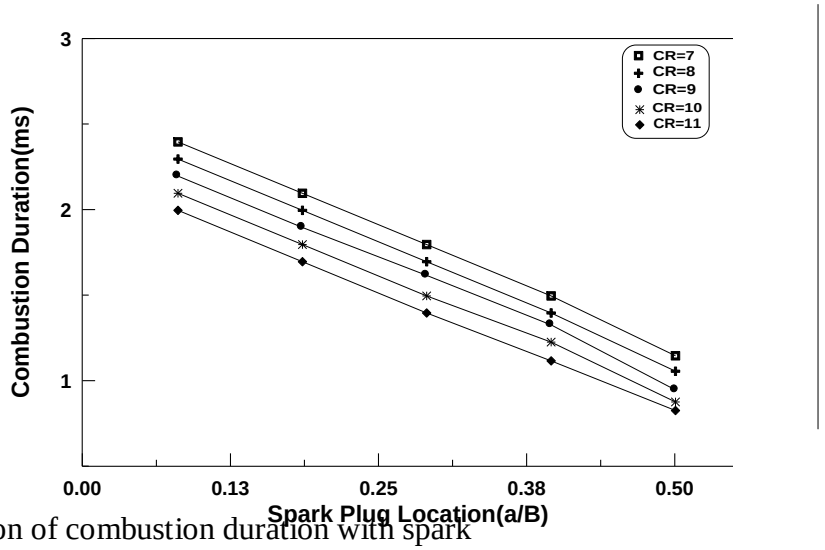

Fig.(5):Variation of combustion duration with spark plug location at different compression ratios.
Engine Speed=2000,Φ =1

CONCLOSION

Spark plug location has a significant effect on both combustion process and emission characteristics of the engine and has to be carefully designed.

The results characterize that the value of cylinder pressure, temperature field, flame speed, and NOx and CO emissions are affected by the spark plug location.

The position of the spark plug have a strong effect on the burning time duration. Shifting the spark plug from central position reduces all studied parameters.

REFRENCES

H.N. Gupta and J.A. Yamin, "The Effect of Combustion Duration on the Performance and Emission Characteristics of Propane-Fueled 4-Stroke S.I. Engines", Emirates Journal for Engineering Research,8(1),1-14(2003).

J.B. Heywood, "Internal Combustion Engine Fundamentals", 1988.

J.B. Heywood, "Combustion and its Modeling in Spark-Ignition Engine", International Symposium COMODIA94 (1994).

Lavoie, G.A. and J.B. Heywood, "Experimental and Theoretical Investigation of Nitric Oxide Formation in Internal Combustion Engine", Combustion Science Technology, Vol.1, pp. 313-326, 1970.

M.R. Razavi, "The Effect of Spark Plug Position on Spark Ignition Combustion ", Faculty of Engineering, Ferdowsi University of Mashhad Iran (2002).

Peter O. Witze, "The Effect of Spark Location on Combustion in a Variable-Swirl Engine", SAE, paper 820044, 1982.

W.J.D. Annand, "Geometry of Spherical Flame Propagation in a Disk-Shaped Combustion Chamber", Journal of Mechanical Engineering Science, Vol.12, no.2, 1970.

Zhichao, T. ,and Rolf, D. Reitz, "Development of G-Equation Combustion Model for Direct Injection SI Engine Simulations", SAE, PP. 01-0722, 2003.

APPENDIX(A)

Engine Specification

Engine Type	(4-Stroke, Spark Engine)
Bore	800 mm
Stroke	1100 mm
Connected Rod Length	243 mm
Intake Valve Timing (Deg.Crank Angle)	Opens 16 BTDC
	Close 40 ABDC
Exhaust Valve Timing (Deg.Crank Angle)	Opens 42 BBDC
	Close 16 ATDC

NOMENCLTURE

The following symbols are used generally throughout the text. Others are defined as when used.

Symbol	Description	Unit
A	Total area of cylinder	m^2
B	Bore	m
C_P	Specific heat at constant pressure	kJ/kg.K
C_V	Specific heat at constant volume	kJ/kg.K
N	Total mole of mixture or products	Mole
P	Pressure	N/m^2
R_{mol}	Universal gas constant	kJ/kg.mol.K
T	Temperature	K
t	Time	sec
V	Volume	M^3
X_i	Mole fraction of species i	Mole of species i/total mole

Subscripts	
a	Air
b	Burned
f	Flame
ht	Heat Transfer
T	Total
u	Unburned
v	Constant volume